

MULTIDIMENSIONAL NLTE RADIATIVE TRANSFER

L. Léger¹, F. Paletou¹ and F. Navarre¹

Abstract. We present the main capabilities and performances of a new 2D numerical radiative transfer code (Léger et al. 2007). It treats self-consistently the radiative transfer and the NLTE statistical equilibrium of H. It includes also the possibility of modelling moving 2D structures such as eruptive prominences.

1 Introduction

Multi-dimensional radiative transfer is of general interest in various domains of astrophysics. Our primary interest concerns the radiative modelling of isolated and illuminated structures in which non-LTE plasma conditions prevail: solar prominences. In particular, spectral lines of He I are commonly used for the diagnosis of the magnetic field of solar prominences. Inversion codes assume so far that spectral lines such as D_3 or 1083 nm for instance are optically thin, which is in fact not always confirmed observationally. Moreover, we suspect that geometry effects also have an impact on the formation of such moderately thick lines (Paletou 1997). This makes therefore necessary the development of new numerical tools for a complete diagnosis of the observations. We have thus developed a new 2D numerical radiative transfer code (Léger et al. 2007). It treats self-consistently the transfer and the NLTE statistical equilibrium of H, so far; it includes also the possibility of modelling moving 2D structures such as eruptive prominences. The implementation of a detailed He model is on progress. Hereafter we present the main performances of our new code.

2 About solar prominences and He I spectrum.

Solar prominences are dense ($n_H \sim 10^{10} \text{ cm}^{-3}$) and cool structures ($\sim 10\,000 \text{ K}$) in the hot ($\sim 10^6 \text{ K}$) and low density ($n_H \sim 10^8 \text{ cm}^{-3}$) corona. They are related to Coronal Mass Ejections (CME) which are huge eruptive phenomena affecting Sun-Earth relations (Subramanian & Dere 2001), and the magnetic field is very likely to play a major role in the triggering of those instabilities leading to the onset of the CMEs.

He I lines such as D_3 line (587.6 nm) and 1083 nm are among the best tools to study the magnetic field in solar prominences. Full-Stokes observations of these spectral lines at THÉMIS (Paletou et al. 2001) have lead to a recent revision of magnetic field inversion tools in particular, by the addition of V (circular) polarization analysis (López Ariste & Casini 2002).

Recent models (Labrosse & Gouttebroze 2001, 2004) assume 1D static layers and no fine structure for the He I model-atom (which leads to gaussian profiles), whereas inversion tools assume that D_3 line is optically thin. But the fine structure is well resolved with present solar spectrographs and leads to different peaks in the line profiles. Measurement of the ratio between these peaks gives a quite direct indication of the optical thickness of the prominence (López Ariste & Casini 2002).

It is therefore important to use the best numerical radiative transfer methods and a full He I atomic model in 2D geometry in order to improve our ability to compute realistic synthetic spectral line profiles and thus magnetic fields determination.

¹ Laboratoire d'Astrophysique de Toulouse & Tarbes (CNRS/UMR 5572), Université de Toulouse, Observatoire Midi-Pyrénées

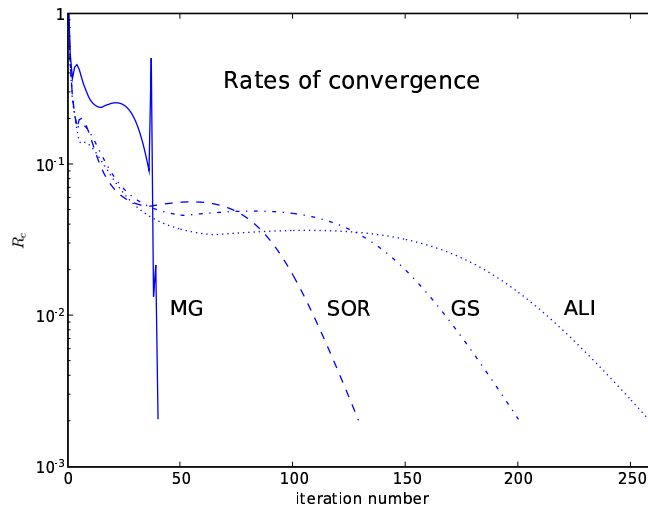


Fig. 1. Maximum relative change R_c on the populations from an iteration to another against the number of iterations for four different numerical methods, showing the great superiority of the MG scheme with a gain of ~ 7 in the iteration numbers against ALI scheme.

3 Numerical radiative transfer: GS/SOR with a multigrid strategy.

While in 1D, only the horizontal thickness of the slab is finite, the 2D geometrical model of a prominence consists of an isothermal and isobaric slab standing horizontally above the chromosphere and illuminated on both sides, and bottom from below, by the chromospheric radiation. In the case of He modelling, the 2D geometry allows also for a more realistic account of the important coronal illumination (Fontenla et al. 1993, Mauas et al. 2005).

The general difficulty in non-LTE radiative transfer for multilevel atoms is to determine the population densities via the resolution of N_{levels} equations of statistical equilibrium (ESE) considering a radiative field (which depends on these populations through N_{trans} radiative transfer equations), and at all grid points of the atmosphere. We use the following scheme :

- the formal solution of the radiative transfer equation is solved in 2D using the SC (short characteristics) method of Auer & Paletou (1994).
- to improve convergence rates, we use a Gauss-Seidel iterative scheme with Successive Over-Relaxation GS/SOR for multilevel atoms (Paletou & Léger 2007).
- finally we include this 2D-GS/SOR iterative scheme into a nested multigrid method (Fabiani Bendicho et al. 1994, Léger et al. 2007).

The numerical procedure is first to solve the statistical equilibrium and the radiative transfer equations for the hydrogen atom and then to solve these equations for the helium atom consistently with the ionization equilibrium computed for hydrogen.

With our code, we can also model moving 2D structures such as eruptive prominences, considering so far a constant radial velocity for the slab.

4 Illustrative examples and results.

We considered a plasma composed of neutral and ionized hydrogen, and neutral helium. The helium abundance is taken equal to 0.1. We adopt a temperature $T = 8000 K$, a gas pressure $p_g = 0.05 \text{ dyn cm}^{-2}$ and a microturbulent velocity $\xi = 5 \text{ km s}^{-1}$. The geometrical width of the slab is $D_y = 5000 \text{ km}$ and its height $D_z = 30000 \text{ km}$, the grid is 243×243 points. We consider 5 bound levels and the continuum for hydrogen.

Table 1. Computing time and number of iterations for four different numerical methods and two spatial grids, showing that MG scheme is not only superior in iteration numbers but also in computing time, especially when the grid is increasingly refined.

Grid points	MALI 2D	GSM 2D	SOR 2D	MG 2D
163x163	184min29s (156)	120min27s (123)	78min41s (84)	31min46s (29)
243x243	698min38s (259)	417min24s (201)	269min21s (130)	65min31s (41)

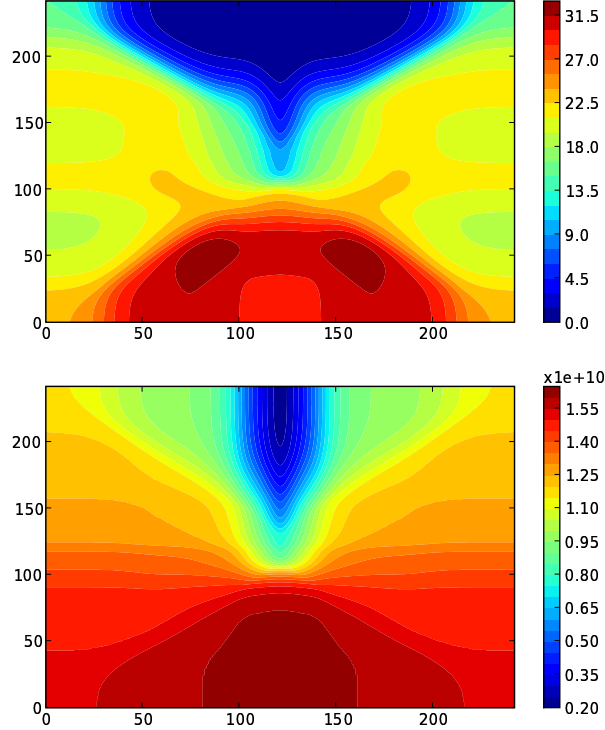


Fig. 2. Contour plots of the first excited level populations normalized to their LTE values n_2/n_2^* (top) and the electronic density n_e (bottom), showing both departures from LTE and geometry effects within the slab. Width (horizontal axis) and height (vertical axis) of the slab are in geometrical point index.

The respective rates of convergence for the ALI, Gauss-Seidel (GS), SOR and Multigrid (MG) multilevel iterative processes in 2D geometry are displayed in Fig. 1 where we plot the maximum relative change R_c on the populations from an iteration to another against the number of iterations. In Tab. 1 we provide the corresponding computing time and number of iterations for two different grids. This shows that the MG scheme is superior in iteration numbers and computing time against all other numerical schemes, especially when the grid is more and more refined¹.

Figures 2 are contour plots of the first excited level populations normalized to their LTE values n_2/n_2^* (top) and the electronic density n_e (bottom). They show both departures from LTE and geometry effects within the slab.

¹this is important for the sake of precision as discussed by Chevallier et al. 2003

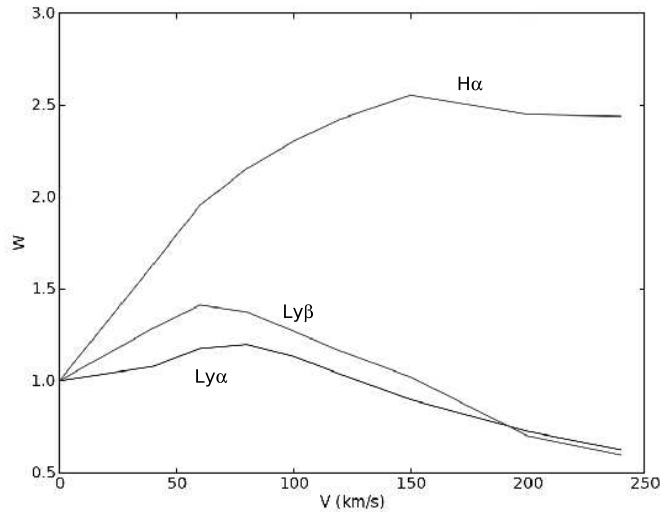


Fig. 3. 2D variations of W against the radial escape velocity V , showing Doppler brightening and dimming for $\text{Ly}\alpha$, $\text{Ly}\beta$ and $\text{H}\alpha$ of H I atom.

Concerning moving prominences, which have not been modelled in 2D so far, Fig. 3 gives the 2D variations of

$$W = \frac{E(V)}{E(V=0)}$$

where E is the spectrally integrated line profile as a function of the macroscopic radial escape velocity V in km.s^{-1} for $\text{Ly}\alpha$, $\text{Ly}\beta$ and $\text{H}\alpha$. A temperature $T = 10\,000\text{ K}$, a gas pressure $p_g = 0.1\text{ dyn cm}^{-2}$ and a microturbulent velocity $\xi = 0.1\text{ km s}^{-1}$ were used. The geometrical width of the slab is $D_y = 1\,000\text{ km}$ and its height $D_z = 100\,000\text{ km}$. We find, in such a case, the same behaviour for Doppler brightening and dimming as in 1D geometry.

Ongoing work is to model a full He I atomic model including the fine structure (D_3 is a “transition” between levels $2^3P_{0,1,2}$ and $3^3D_{1,2,3}$ for instance). Indeed considering fine structure is critical in order to fully exploit high spectral resolution spectropolarimetric measurements we are collecting with the THÉMIS solar telescope in the visible and near infrared simultaneously.

References

- Auer, L.H., & Paletou, F. 1994, A&A, 285, 675
 Chevallier, L., Paletou, F. & Rutily, B. 2003, A & A, 411, 221
 Fabiani Bendicho, P., Trujillo Bueno, J. 2001, Auer, L., 1997, A&A, 324, 161
 Fontenla, J.M., Avrett, E.H. & Loeser, R. 1993, ApJ, 406, 319
 Labrosse, N., & Gouttebroze, P. 2001, A&A, 380, 323
 Labrosse, N., & Gouttebroze, P. 2004, ApJ, 617, 614
 Léger, L., Chevallier, L. & Paletou, F. 2007, A&A, 470, 1
 López Ariste, A. & Casini, R. 2002, ApJ, 575, 529
 Mauas, P.J.D., Andretta, V., Falchi, A., Falciani, R., Teriaca, L. & Cauzzi, G. 2005, ApJ, 619, 604
 Paletou, F. 1995, A&A, 302, 587
 Paletou, F. 1997, A&A, 317, 244
 Paletou, F., & Léger, L. 2007, JQSRT, 103, 57
 Paletou, F., López Ariste, A., Bommier, V., & Semel, M. 2001, A&A, 375, 39
 Rybicki, G. B., & Hummer, D. G. 1992, A&A, 245, 171
 Subramanian, P., & Dere, K.P. 2001, ApJ, 561, 372